PREPARING 3D GRAPHENE NANOWALL-NICKEL HYBRID ELECTRODE ON QUARTZ GLASS FOR ON-CHIP MICRO-SUPERCAPACITORS

Jinhua Li, and Takahito Ono
Graduate School of Engineering, Tohoku University, Sendai, JAPAN

ABSTRACT

We report a type of MEMS-technique processable micro-supercapacitors built on 3D graphene nanowall (GNW)/Ni core-shell electrodes. While the growth of GNW on quartz glass and other conductive substrates were rationally revealed, the microfabrication of hybrid electrodes was realized by uniformly coating Ni on GNW to simultaneously serve as a shadow mask for patterning and an active material for capacitance augmentation. With 10-fold larger capacitance of 337 F/cm^3 than that using pure GNW and Ni, the core-shell electrodes enabled a high on-chip energy and power density delivery of the capacitor. The non-catalytic growth and micromachining strategy possibly promote applying GNW in various microsystems.

INTRODUCTION

Recently, the versatile and highly integrated trends of wearable electronics raise increasing demands on supporting energy storage devices with tremendous power supply and on-chip processability through MEMS fabrication technique. Micro-supercapacitors (MSCs) is a desirable power source candidate to render high-performance exceeding its bulk counterparts and the thin-film batteries by benefiting from a shorter electrolyte ion migration path and surface electrochemical reaction essence [1]. Many previous researches demonstrated several types of MSCs based on either pristine planar graphene or its composites with pseudo-capacitive (i.e. transition metal oxides, hydroxides, conjugated polymers) nanomaterials by leveraging the huge surface and electric conductive nature of graphene [2]. Nevertheless, most of the MSCs display achievable energy density in a poor range less than 1 mWh/cm^3 and an electrochemical properties loss, which is owing to the inefficient surface utilizing caused by strong inter-plane restacking tendency of graphene layers [3]. In contrast to the horizontally oriented planar graphene, the morphology of GNW with vertically aligned interconnect few-layer graphene is more stable, while its distinct ordered 3D structure enables an ideal bi-continuous networks for electron transfer and an accessible surface for electrolyte diffusion [4]. Although incorporate GNW with those pseudo-capacitive materials as the microelectrodes of MSCs may trigger an unprecedented energy storage performance delivery, a compatible microfabrication method on wafer substrates and the approach to evenly coat active nanomaterials on GNW have rarely been studied. In addition to the device fabrication itself, in-depth investigation of the GNW growth on diverse substrates may profoundly advance the applications of GNW in various MEMS devices, such as sensors, field-emitters, and photo-detectors, etc.

In this work, we present a MSCs built on 3D GNW/Ni core-shell hybrid electrodes. While a non-catalytic direct synthesis of GNW on both dielectric insulating (i.e. quartz glass) and conductive substrates were rationally discussed, a suitable micromachining route of GNW/Ni hybrids was also demonstrated for the first time. Electrochemical evaluation indicated a high energy and power density of the MSCs, which mainly originated from the excellent performance of novel core-shell hybrid electrodes.

EXPERIMENTAL SECTION

Synthesis of GNW on different substrates

GNW thin-film was produced by a catalyst-free direct growth method through a microwave plasma enhanced chemical vapor deposition (MPECVD) with the gas reactants of H_2 and CH_4 (Figure 1). A quartz glass with size of 1 cm^2 was used as the substrate. Briefly, the substrate was uplifted by a ceramic support at the stage height of ~50 mm and exposed to 750 W plasma for a period of pre-treatment under 50 sccm flow of H_2. Afterwards, 10 sccm flow of CH_4 was introduced to initiate the GNW growth. During the whole deposition, the CH_4/H_2 flow ratio was maintained at 1:5 with total chamber pressure at 30 torr. Due to the strong plasma-induced heating, no extra substrate heating was required. After 30 min deposition, the plasma and gas flow were switched off and followed by 2 hours natural cooling. Other dielectric insulators (i.e. Al_2O_3) and conductive wafers (i.e. Pt, Si) were also examined for evaluating the synthesis conditions of GNW on different substrates.

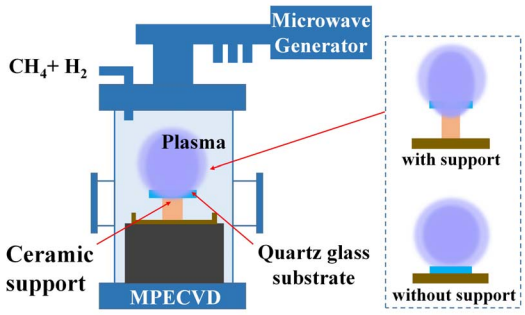

Figure 1: Illustration of experimental setup and the plasma shape difference with and without a ceramic support for GNW growth via MPECVD.

Microfabrication of GNW/Ni core-shell hybrid MSCs

The MSCs based on GNW/Ni core-shell electrode was fabricated on quartz glass (Figure 2). (1) Interdigitated electrodes of Ti-Pt (20nm/280nm-thick) was designed as the current collector via lift-off process. (2) The GNW was synthesized to cover the whole substrate surface by the MPECVD method. (3) About 150 nm-thick Ni was deposited

on the as-obtained GNW via the electron beam evaporation (EB). (4) Alignment and photolithography were performed to define the microelectrodes area while the exposed Ni was etched by ferric chloride solution to leave behind the shadow mask pattern. (5) The MSCs was generated by removing the exposed GNW through the reactive ion etching (RIE) under 100W plasma with 10 Pa pressure at 50 sccm O_2 flow. (6) Electrochemical activation of the as-obtained hybrid electrodes was carried out by sweeping 30-cycles at -0.9~0.9 V range in 6M KOH solution to convert the GNW/Ni to GNW/$Ni(OH)_2$.

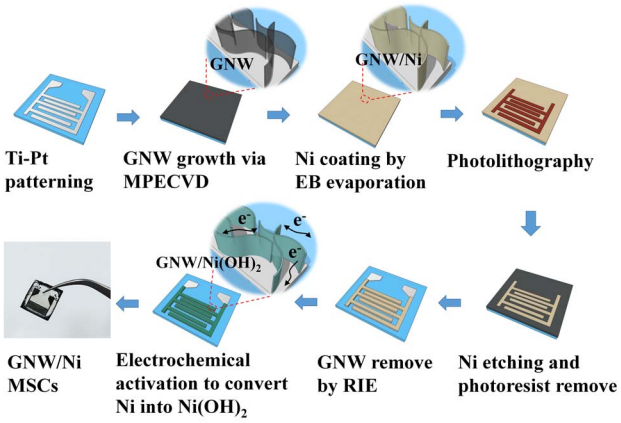

Figure 2: The schematic view of the process for GNW/Ni core-shell hybrid MSCs fabrication.

RESULTS AND DISCUSSIONS

Growth of GNW on various substrates

In this work, the GNW can be directly synthesized on a quartz glass and other dielectric or conductive substrates (i.e. Al_2O_3, Si, Pt) through the MPECVD method without using a catalyst, which eliminate the needs for complex post-transfer. The MPECVD generally produces high density plasmas and enables the growth of GNW experienced three periods [5]. At first, H_2 plasma pretreatment rapidly warms-up the substrate surface to high-temperature and the plasma bombardment creates surface defects for trapping the dissociated carbon species. Then, nucleation occurs at the defect spots while large stress forms in the nucleus and facilitates anisotropic growth of carbon nanostructures in the presence of plasma electric field. The much higher etching rate of amorphous carbon than sp^2 carbon under H_2 plasma lead to the nanostructures of graphitic phase. Finally, further absorption of carbon species on the as-formed graphite nanostructures enables continuous erect growth of nanowall-like graphene.

It is noteworthy that elevating the substrates with a ceramic support is the key to successfully depositing GNW. A clear shape difference of plasma ball were observed with/without ceramic support during experiment (Figure 1). It is believed that the isolation of substrates from the chamber stage by using ceramic not only help focus plasma and immerse the substrate into plasma region for an effective plasma-surface coupling, but also can impede the thermal conduction from the sample surface to the stage and avoid large amount of heat loss.

The SEM graphs (Figure 3) indicate the morphology of GNW with average height of ~1 μm on different substrates. The free-standing graphene display typical vertically aligned feature and well connected with each other to form continuous 3D networks. Plasma pretreatment duration can influence the nucleation stage and thus control the GNW deposition rate, which was found to be vary with the substrate types. As shown in Figure 3e, longer pretreating time were required to synthesize ~1 μm-thick GNW film on quartz glass and Al_2O_3 than those on Si and Pt substrates under identical 750 W plasma and 30min effective deposition duration. This may be governed by the substrate conductivity, surface roughness and catalytic effect. In contrast to the Pt and Si, it is inferred that the poor conductivity of quartz glass and Al_2O_3 can cause surface charge accumulation and build reverse electric field [6] to reduce surrounding plasma density. A relative smooth quartz glass surface suggests that a longer-term plasma bombardment is necessary to create surface defects for carbon species capture. The possible catalytic effect on carbon species dissociation from Pt may be another reason for the ease of GNW growth [7].

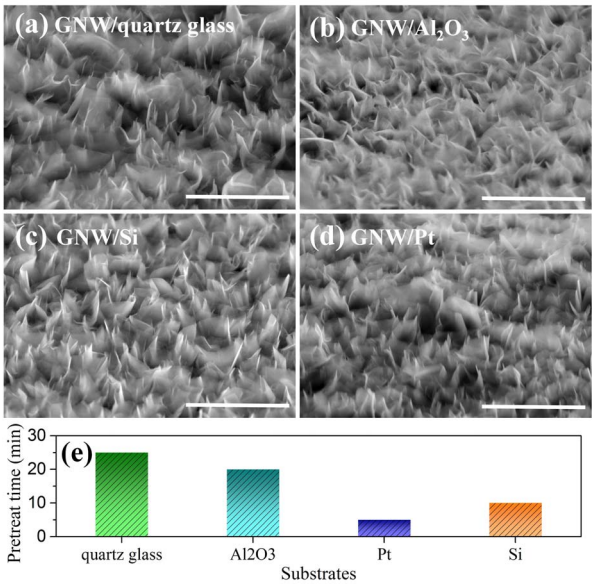

Figure 3: SEM images of GNW growth on (a) quartz glass (b) Al_2O_3 ceramic (c) Si and (d) Pt surface. The scale bar: 3 μm. (e) The H_2 plasma pretreatment time for ~1 μm-thick GNW film growing on different substrates.

Fabrication of GNW/Ni core-shell hybrid MSCs

The MSCs was designed with electrodes of GNW scaffold and supported Ni-based pseudo-capacitive material. To overcome the challenge of uniformly coating active materials in porous nanostructures, the EB evaporation was utilized to deposit Ni onto the individual GNW nanosheet by considering its physical vapor deposition essence of this method with easily controllable coating rate. Figures 4a and 4b show the GNW morphology consisted of free-standing

graphene sheets on the quartz glass. After ~150 nm-thick Ni layer evaporation, the thickened graphene layers are found to be evenly coated with visible thin-films (Figures 4c and 4d). It is noteworthy that the Ni layer served two main roles here as both a shadow mask layer for electrodes micro-patterning and the precursors which can be in-situ converted into $Ni(OH)_2$ active material by an electrochemical activation. Moreover, the as-deposited Ni was also believed to protect the GNW from the external damage during photolithography. If not, the viscous photoresist in spin-coating and the large capillary force during drying after development can easily destroy or collapse the structures of GNW.

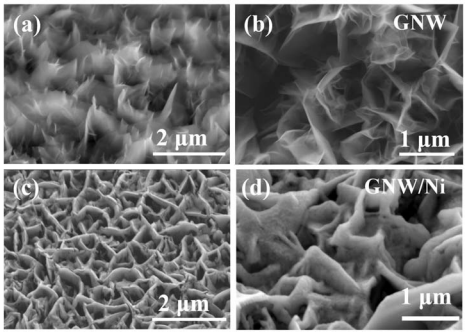

Figure 4: SEM images of (a) GNW as-deposited on quartz glass and (c) after Ni coating by EB evaporation. (b) and (d) indicate the magnification of (a) and (c), respectively.

The electrochemical activation of the as-fabricated GNW/Ni microelectrodes was performed in 6M KOH solution through a three-electrode setup. With Pt wire and Ag/AgCl as the counter and reference electrodes, respectively, the hybrid electrode was electrochemically oxidized under a sweeping from -0.9 to 0.9 V for 30 circles. It is found from the SEM insets in Figure 5 that the activation coarsened the GNW/Ni surface and created flower-like nanostructures. It is attributed to a crystalline transition and volume swelling during the conversion from Ni to $Ni(OH)_2$ and NiOOH through the electrochemical reactions [8]:

$$Ni + 2OH^- \rightarrow Ni(OH)_2 + 2e^- \quad (1)$$

$$Ni(OH)_2 + OH^- \leftrightarrow NiOOH + H_2O + e^- \quad (2)$$

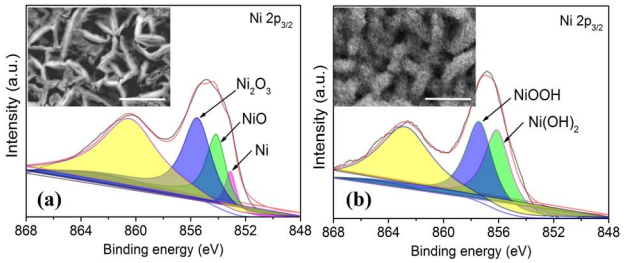

Figure 5: XPS analysis of GNW/Ni electrodes (a) before and (b) after electrochemical activation. The insets are the corresponding SEM images at the scale bar of 1 µm.

This is also proofed by the XPS spectrum analysis in Figure 5. While the Ni $2p_{3/2}$ peaks [9] at 852.7 eV, 854.1 eV, 855.4 eV indicate the existence of Ni, NiO and Ni_2O_3 on the hybrid electrode surface before activation, the blue shift of peaks with missing metallic Ni signal in Figure 5b indexes the transition of Ni at GNW surface into the $Ni(OH)_2$ and NiOOH after electrochemical oxidation.

Electrochemical energy storage evaluation of the GNW/Ni hybrid electrodes and MSCs

Electrochemical performance of the GNW/Ni hybrid electrodes was determined by cyclic voltammetry (CV) in the three-electrode test. It is found (Figure 6a) that the hybrid electrodes behave in a typical faradaic redox CV curves with highly symmetric and large CV window even at the scan rate of 200 mV/s, which was governed by the reversible transition between $Ni(OH)_2$ and NiOOH at electrode surfaces. The CV profile suggests an excellent capacitance up to 337 F/cm^3, which is more than 10-times higher than that of pristine GNW and Ni electrodes counterparts.

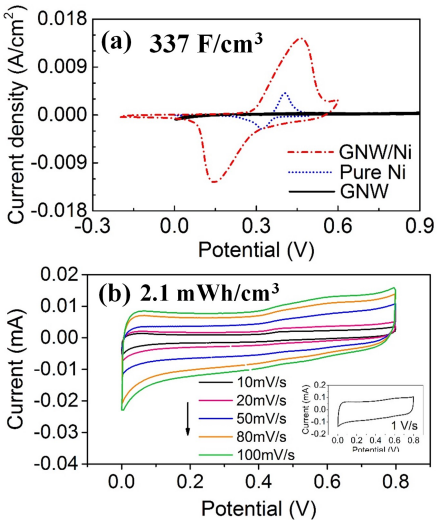

Figure 6: (a) CV analysis of GNW/Ni electrodes compared to that of pure GNW and Ni at 200mV/s scan. (b) The CV curves of MSCs versus different scan rates.

In addition, a two-electrode test was further performed to examine the performance of the MSCs. As depicted in Figure 6b, the MSCs show symmetric and rectangular-like CV profiles at the scan rates of 10~1000 mV/s, suggesting an exceptional electrochemical reaction kinetics and a high-rate capability of the device.

Calculation from the CV data verified that our MSCs with a high stack energy density up to 2.1 mWh/cm^3 and maximum power density of 5.91 W/cm^3. As it compared in Figure 7a, our MSCs suggests a superior energy storage ability that outperforms other reported researches and displays 2-order higher energy and power density delivery than the commercial capacitors and thin-film lithium batteries, respectively [1, 3, 10-13]. Meanwhile, the long-term operation stability and galvanostatic charge/discharge behaviors of the MSCs were also studied (Figure 7b). It is found that the device can retain 96%

capacitance after 2000-cycles operations under 50 mV/s scan. The inset charge/discharge plot shows a symmetric quasi-triangular feature, implies a relative good electrochemical reversibility of the MSCs. Such remarkable performance can be primarily owing to the distinct structures of GNW/Ni core-shell hybrid electrodes. The 3D network of GNW scaffold rendered bi-continuous pathway for charge transport and offered huge accessible areas to support Ni pseudo-active material for abundant surface redox reactions.

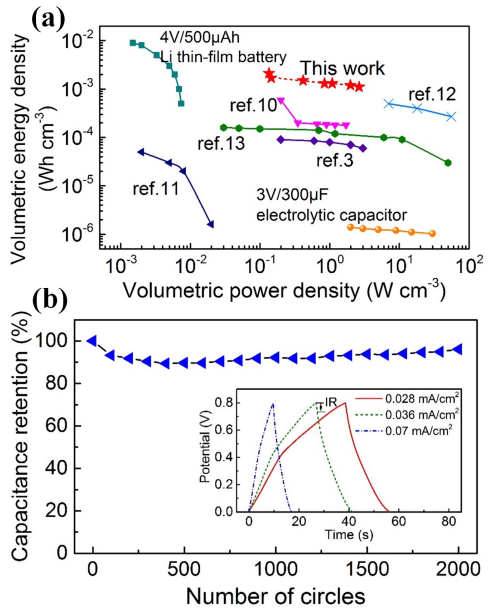

Figure 7: (a) Ragone plot of the MSCs performance with comparison to other reported works. (b) Cycling stability and galvanostatic charge/discharge (inset) plot of the MSCs.

CONCLUSIONS

We prepared a micro-supercapacitors based on 3D GNW/ Ni core-shell electrodes through MEMS process. As the growth of GNW on insulating and conductive substrates were rationally discussed, the microfabrication of the hybrid microelectrodes was realized by uniformly coating Ni on GNW to simultaneously serve as shadow mask for patterning and an active material for capacitance improvement. With 10-fold larger capacitance than that using pure GNW and Ni, the novel core-shell electrodes enable an excellent on-chip energy and power density delivery of the capacitors. The non-catalytic direct GNW growth on different substrates and the compatible micromachining strategy may shed a new light for applying GNW in various functional microsystems.

REFERENCES

[1] D. Pech, M. Brunet, H. Durou, P. Huang, V. Mochalin, Y. Gogotsi, P. Taberna, P. Simon, "Ultrahigh-Power Micromete-Sized Supercapacitors Based on Onion-Like Carbon", *Nat. Nanotechnol.,* vol. 5, pp. 651-654, 2010.

[2] M. Beidaghi, Y. Gogotsi, "Capacitive Energy Storage in Micro-Scale Devices: Recent Advances in Design and Fabrication of Micro-supercapacitors", *Energy. Environ. Sci.,* vol. 7, pp. 867-884, 2014.

[3] M. El-Kady, V. Strong, S. Dubin, R. Kaner, "Laser Scribing of High-performance and Flexible Graphene-Based Electrochemical Capacitors", *Science,* vol. 335, pp. 1326-1330, 2012.

[4] Q. Liao, N. Li, S. Jin, G. Yang, C. Wang, "All-Solid-State Symmetric Supercapacitor Based on Co_3O_4 Nanoparticles on Vertically Aligned Graphene", *ACS Nano,* vol. 9, pp. 5310-5317, 2015.

[5] N. Soin, S. Roy, T. Lim, J. McLaughlin, "Microstructural and Electrochemical Properties of Vertically Aligned Few Layered Graphene (FLG) Nanoflakes and Their Application in Methanol Oxidation", *Mater. Chem. Phys.,* vol. 129, pp. 1051-1057, 2011.

[6] G.A. Emmert, "Model for Expanding Sheaths and Surface Charging at Dielectric Surfaces During Plasma Source Ion Implantation", *J. Vac. Sci. Technol. B,* vol. 12, pp. 880-883, 1994.

[7] L. Gao, W. Ren, H. Xu, L. Jin, Z. Wang, T. Ma, L. Ma, Z. Zhang, Q. Fu, L. Peng, X. Bao, H. Cheng, "Repeated Growth and Bubbling Transfer of Graphene with Millimeter-Size Single-Crystal Grains Using Platinum", *Nat. Commun.,* vol. 3, pp. 699, 2012.

[8] Y. Jiang, P. Wang, X. Zang, Y. Yang, A. Kozinda, L. Lin, "Uniformly Embedded Metal Oxide Nanoparticles in Vertically Aligned Carbon Nanotube Forests as Pseudocapacitor Electrodes for Enhanced Energy Storage", *Nano Lett.,* vol. 13, pp. 3524-3530, 2013.

[9] A. Dutta, J. Datta, "Energy Efficient Role of Ni/NiO in PdNi Nano Catalyst Used in Alkaline DEFC", *J. Mater. Chem. A,* vol. 9, pp. 3237-3250, 2014.

[10] H. Wu, K. Jiang, S. Gu, H. Yang, Z. Lou, D. Chen, G. Shen, "Two-Dimensional $Ni(OH)_2$ Nanoplates for Flexible On-Chip Microsupercapacitors", *Nano Res.,* vol. 8, pp. 3544-3552, 2015.

[11] P. Huang, X. Xiao, Y. Li, Y. Ding, P. Qiang, X. Tan, W. Mai, Z. Lin, W. Wu, T. Li, H. Jin, P. Liu, J. Zhou, C. Wong, Z. Wang, "Hydrogenated ZnO Core-Shell Nanocables for Flexible Supercapacitors and Self-Powered Systems", *ACS Nano,* vol. 7, pp. 2617-2626, 2013.

[12] K. Grigoras, J. Keskinen, L. Groneberg, E. Yli-Rantala, S. Laakso, H. Vaelimaeki, P. Kauranen, J. Ahopelto, M. Prunnila, "Conformal Titanium Nitride in A Porous Silicon Matrix: A Nanomaterial for In-Chip Supercapacitors", *Nano Energy,* vol. 26, pp. 340-345, 2016.

[13] J. Lin, C. Zhang, Z. Yan, Y. Zhu, Z. Peng, R. Hauge, D. Natelson, J. Tour, "3-Dimensional Graphene Carbon Nanotube Carpet-Based Microsupercapacitors with High Electrochemical Performance", *Nano Lett.,* vol. 13, pp. 72-78, 2013.

CONTACT

*J.H. Li, tel: +81-22-795-5806;
jhli@nme.mech.tohoku.ac.jp